Liquid Crystals
Publication details, including instructions for authors and subscription information:
http://www.informaworld.com/smpp/title~content=t713926090

Soft mode and related behaviour in the SmA and SmC* phases of a ferroelectric liquid crystalline polymer by dielectric spectroscopy

S. K. Kundu; B. K. Chaudhuri; L. Catala; S. Mery

To cite this Article Kundu, S. K. , Chaudhuri, B. K. , Catala, L. and Mery, S.(2002) 'Soft mode and related behaviour in the SmA and SmC* phases of a ferroelectric liquid crystalline polymer by dielectric spectroscopy', Liquid Crystals, 29: 6, 837 — 842

To link to this Article: DOI: 10.1080/02678290210133123

URL: http://dx.doi.org/10.1080/02678290210133123

LIQUID CRYSTALS, 2002, VOL. 29, NO. 6, 837–842

Taylor & Francis
Taylor & Francis Group

Soft mode and related behaviour in the SmA and SmC* phases of a ferroelectric liquid crystalline polymer by dielectric spectroscopy

S. K. KUNDU, B. K. CHAUDHURI*
Solid State Physics Department,
Indian Association for the Cultivation of Science, Calcutta-700032, India

L. CATALA and S. MERY
Institut de Physique et Chemie des Materiaux de Strasbourg,
Groupe des Materiaux Organiques, 23 rue Loess, 67037 Strasbourg Codex, France

(*Received 15 October 2001; in final form 15 January 2002; accepted 26 January 2002*)

Anomalous dielectric relaxation behaviour is observed in the ferroelectric liquid crystalline polymer (viz. ferroelectric copolysiloxane (R)-COPS 11-10) around the ferroelectric SmC* to paraelectric SmA phase transition. Measurements have been performed on sample of thickness ~10 μm in indium-tin-oxide coated cell in the frequency range 10 Hz to 13 MHz. With increase of temperature, a gradual shift of the soft mode frequency towards the higher frequency side was observed, while a decrease in the relaxation strength was seen with the corresponding increase in temperature. The shifts of the soft modes in the SmC* and SmA phase are considered to be due to change in the viscosity of the polymer, as an increase in viscosity increases fluctuations of the coupling between the dipoles in the network even far from the paraelectric–ferroelectric phase transition. Application of a bias field causes a shift of the critical frequency towards the higher frequency side, while the dielectric strength ($\Delta\varepsilon$) decreases under the bias field. The Cole–Cole fitting parameters obtained from the best fit of the dielectric constant data are found to be consistent with other similar materials. Another relaxation mode (molecular mode) was also observed which comes into play in both the smectic phases (SmC* and SmA) and contributes to the dielectric permittivity.

1. Introduction

The study of liquid crystalline polymers is a stimulating field of current research because of their applications in optoelectronics and other devices. However, successful demonstration of the behaviour of ferroelectric liquid crystalline polymers (FLCPs) is a rather recent development in polymer science [1]. In recent years, several new polymer structures have been reported [2–6] as showing both ferroelectric SmC* and paraelectric SmA phases. It is generally considered that the SmA–SmC* transition is due especially to softening of the inhomogeneous fluctuations of the molecular tilt with respect to the normal to the smectic layer when the transition is approached from the SmA phase. In the ferroelectric phase, a spontaneous tilt of the molecules appears, the directions of which precess about the smectic normal, and a helicoidal structure is formed. It is well known that studies [7, 8] of dielectric relaxation behaviour in liquid crystals provide valuable information regarding the dipolar response to an external stimulus. However, in many such FLCP systems it is rather difficult to measure dielectric constants because of high viscosity and melting point.

Dielectric relaxation measurements of the collective modes in ferroelectric liquid crystals (FLCs) in the SmC* and SmA phases indicate two main modes, viz. the Goldstone mode (G-mode, [9–11] and the soft mode (S-mode) [11–15]). The G-mode in the SmC* phase arises due to phase fluctuations of the azimuthal orientation of the director, while the S-mode appears due to fluctuation of the amplitude of the tilt angle. In 1987 however Levstik *et al.* [16] showed theoretically as well as experimentally that in some FLC mixtures, the S-mode can appear in both the SmC* and SmA phases (very close to the SmC*–SmA transition temperature).

In the present paper we report a broad band dielectric study in the region of the SmC*–SmA phase transition of a recently developed and interesting FLCP showing both S-mode and G-mode behaviour. The system of our present investigation is the ferroelectric copolysiloxane (R)-COPS 11-10 [17] having the molecular formula shown below. All the information regarding the 'chemical' characterization of this polymer can be found in an

---

*Author for correspondence,
e-mail: sspbkc@mahendra.iacs.res.in

Liquid Crystals ISSN 0267-8292 print/ISSN 1366-5855 online © 2002 Taylor & Francis Ltd
http://www.tandf.co.uk/journals
DOI: 10.1080/02678290210133123

earlier publication [17]. The degree of polymerization is about 30, the average number of siloxane monomer repeat units substituted by a mesogen is 38%. The calculated molar mass of this polymer is about 9060. Frequency (10 Hz–10 MHz), temperature (100–130 °C) and bias field (0.0–10.0 V) dependent dielectric properties of this typical FLCP have now been investigated and the experimental data fitted with existing theoretical models. The characteristic features of the relaxation modes have been so evaluated. It is observed that in the present system, the S-mode extends beyond the SmA phase as pointed out by Levstik *et al.* [16] for some ferroelectric liquid crystals.

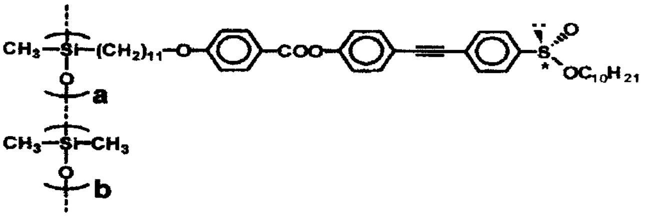

2. Experimental

The method of synthesis of the ferroelectric copolysiloxane (R)-COPS 11-10 of our present investigation has already been discussed by Mery *et al.* [17]. The liquid crystal cell used consisted of parallel indium-tin-oxide (ITO) coated glass plates with an active area of 16 mm^2. A small electrode area was used to minimize the effects of any thickness gradient in the cell and also to ensure a uniform electric field across the sample. The sample was sandwiched between the ITO-coated glass plates, separated by mylar spacers of 10 µm thickness. The glass plates had been treated with a polyimide solution and unidirectionally rubbed for planar alignment. The cell was calibrated using air and pure benzene as a standard reference. This allowed us to obtain the absolute value of dielectric permittivity of the present sample. The sample was introduced into the cell by capillary action in its isotropic phase. The phase sequence (SmX is an unknown phase) of the material used in this study is:

I–164°C–SmA–121°C–SmC*–102°C–SmX

A stabilized low frequency a.c. (1.62 V µm^{-1}) field was used for better alignment of the sample; this was applied for about 75 min. A computer controlled Hewlett Packard 4192A Impedance Analyzer was used for the dielectric measurements in the frequency range 10 Hz–13 MHz. This allowed us to measure the real and imaginary parts of the complex dielectric permittivity ε^* as a function of frequency. The experimental set-up allowed us to apply a direct bias voltage (0.0 to -10.0 V) across the cell during the dielectric measurements. The temperature of the sample was controlled by a Eurotherm temperature controller and the temperature could be stabilized to an accuracy ± 0.1°C. The theoretical procedure discussed below was used to analyse the experimental data.

3. Theoretical background

The complex dielectric permittivity $\varepsilon^*(\omega, t)$ can be expressed by the usual relation

$$\varepsilon^*(\omega, t) = \varepsilon'(\omega, t) - i\varepsilon''(\omega, t) \tag{1}$$

where ε' and ε'' are, respectively, the real and imaginary parts of the dielectric constant, ω is the angular frequency and t is the temperature of the system. For the planar oriented FLCP sample, the possible relaxation modes in the frequency range 10 Hz to 13 MHz are the G-mode, S-mode and molecular mode (M-mode). The observed dielectric spectrum involving orientational relaxation may be studied through the Meier–Saupe and Martin theory [18] of the extended Debye model. However, the dynamic behaviour of the liquid crystal dipole can be determined from the effective analysis as we studied the temperature dependence of the low frequency dispersion. Debye theory of dipole relaxation assumes that rotational motion can be described in terms of a single relaxation time. In real systems, fluctuations in the local structure of the molecule or its environment may result in a distribution of relaxation times around the Debye value, and such a situation can be described by a modified Debye equation. Cole's modified [19] theory of static dielectric permittivity for irreversible processes explains the low frequency dielectric liquid crystal relaxation of our present system. However, the Cole–Cole theory [20] of complex dielectric permittivity is found to be more relevant to the observed off-centred LC dispersions through the equation

$$\varepsilon^* - \varepsilon_\infty = \frac{\Delta\varepsilon}{1 + (i\omega\tau)^{1-\alpha}} \tag{2}$$

where $\Delta\varepsilon = \varepsilon_s - \varepsilon_\infty$ is the dielectric strength, ε_s is the static dielectric constant, ε_∞ is the high frequency dielectric permittivity, $\tau\,(=1/(2\pi f_c))$ is the dielectric relaxation time, f_c is the relaxation peak frequency and α is the distribution parameter. For a distribution of relaxation times, α lies between 0 and 1. The effect of α is to produce a semicircular Cole–Cole plot, the centre of which is depressed below the abscissa. The larger α is, the larger is the extent of the distribution of relaxation times.

It is well known that the contribution of conduction is higher at low frequencies. Its frequency dependence can be expressed [21] by

$$\varepsilon''(\omega) = \frac{\delta_0}{\varepsilon_0 \omega^{1-s}} \tag{3}$$

where δ_0 and s are fit parameters. The power law exponent (s) is generally less than one, indicating a polaron hopping type of conduction mechanism. It appears that the conductivity contribution covers all the processes. However, by taking conductivity into account a qualitative explanation of the relaxation mechanism is possible.

Using the mean field approximations [22], the critical frequency (ν_c^s) of the collective modes should follow the relation:

$$\nu_c^s = a(T - T_C) + b \tag{4}$$

where a and b are constants. These critical frequencies of the collective modes were fitted with the Arrhenius law for the SmC* and SmA phases:

$$\nu_1 = \nu_{\infty 1} \exp\left(\frac{E_a}{k_B T}\right) \tag{5}$$

where $\nu_{\infty 1}$ is a parameter, k_B is the Boltzmann constant and E_a is the activation energy.

4. Results and discussion

Using the above theoretical model, the dielectric absorption spectra of the FLCP sample (ferroelectric copolysiloxane (R)-COPS 11-10) taken over a wide temperature range (100–130°C) were explained and the overall behaviour of the FLCP could be understood. Figure 1 (*a*) shows the variation of the imaginary part of the dielectric constant (ε'') as a function of frequency at different fixed temperatures (110, 112, 116, 119.5 and 120°C) corresponding to the G-mode in the ferroelectric SmC* phase. The G-mode appeared around 103°C and extended to 119.5°C, about 1.5°C below the ferroelectric SmC*–paraelectric SmA phase transition point (~121°C). The G-mode peak frequency is found to be weakly temperature dependent as indicated by this figure. The strength of this relaxation mode decreases with temperature. This is consistent with the behaviour of other similar materials [23]. Figures 1 (*a*) and inset 1 (*b*) also show the dielectric relaxation curves (solid lines) obtained by fitting with the Cole–Cole model, equation (2). From the Cole–Cole plot, we find that the distribution parameter (α) varies from 0.1–0.3. The distribution parameter also produces a semicircular curve, the centre of which is depressed below the abscissa as mentioned in § 3. In the ferroelectric SmC* phase, the S-mode was not observed from 102.5 to 119.5°C.

Near the SmC*–SmA transition temperature (121°C), the G-mode disappeared and the S-mode appeared in the ferroelectric SmC* phase, figure 2 (*a*). The suppression of the G-mode near the transition temperature is due to the low frequency relaxation caused by ions present in this sample. The dotted line in figure 2 (*a*) shows the conductivity contribution by fitting with equation (3). This figure also shows that the variation of the S-mode peak frequency is highly temperature dependent. The soft mode in SmC* phases can be simply explained by

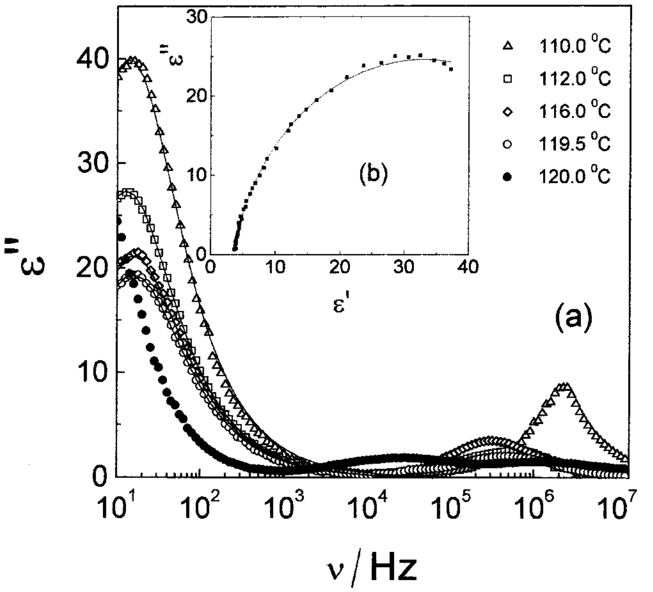

Figure 1. (*a*) Frequency (ν) dependence of the imaginary part of the dielectric constant (ε'') of the G-mode in the ferroelectric SmC* phase at different fixed temperatures. (*b*) Cole–Cole plot obtained for the Goldstone mode in the SmC* phase.

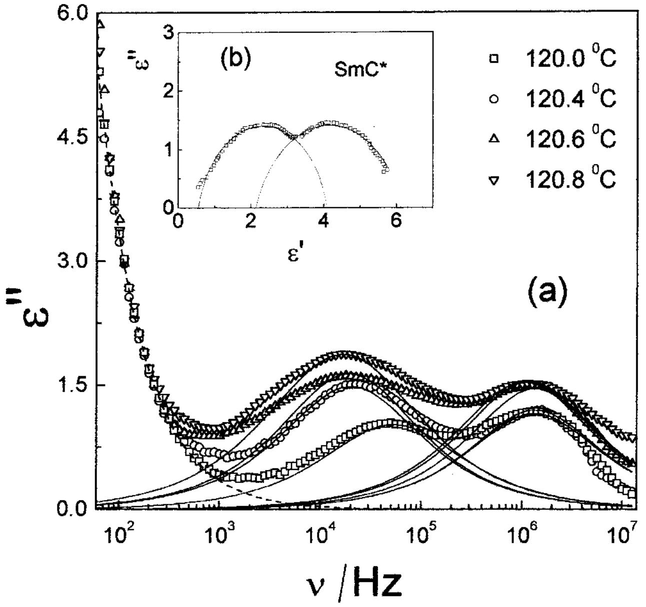

Figure 2. (*a*) Frequency (ν) dependence of the imaginary part of the dielectric constant (ε'') in the ferroelectric SmC* phase at different fixed temperatures. The dotted line shows the conductivity contribution, (using equation (3), with the fit parameters $\delta_0 = 2.56 \times 10^{-11}\ \Omega^{-1}\,\mathrm{cm}^{-1}$ and $s = 0.027$). The solid line shows the Cole–Cole function, equation (2). (*b*) Cole–Cole plot obtained for the soft mode in the SmC* phase.

considering changes in the viscosity in the resulting polymer sample (i.e. the co-operativity of the soft mode fluctuations due to the coupling of dipoles in the network, even far from the phase transition). The solid lines in inset figure 2 represent the Cole–Cole fitting with equation (2).

The dielectric relaxation processes evident in the SmA phase due to the S-mode have been studied using the complex dielectric permittivity ($\varepsilon^* = \varepsilon' - i\varepsilon''$) measured in the frequency range 100 Hz to 13 MHz. The dashed line in figure 3 (*a*) shows the conductivity contribution by fitting with equation (3). This figure shows again that the variation of S-mode peak frequency is highly temperature dependent. Here again the shift of the soft mode in the SmC* and SmA phases can be similarly explained, as mentioned above, by considering change in viscosity. The solid lines in figures 3 (*a*) and inset 3 (*b*) represent the Cole–Cole fitting with equation (2).

From figures 2 and 3, we also observed another relaxation mode which comes into play in both smectic phases (SmC* and SmA). This mode, as mentioned earlier, is considered to be the molecular mode (M-mode). It is well known that in polar liquid crystals, one might visualize two principal molecular orientations, viz. orientations around the short and the long molecular axes. From our experimental data it is clearly seen that both molecular motions contribute to the dielectric permittivity. The critical frequencies of the low frequency molecular relaxation are much higher than those of the G-mode and S-mode relaxation processes, similarly to the situation for ordinary liquid crystal materials studied earlier [24]. The imaginary part of the dielectric constant of this M-mode is also fitted with the Cole–Cole modification, equation (2).

It is seen from the plot of critical frequency as a function of inverse temperature (figure 4) that the thermal variation of G-mode critical frequency is very weak in the temperature range 103 to 119.5°C. The activation energy of the G-mode estimated from equation (5) is about $1.157\,\mathrm{kJ\,mol^{-1}}$ ($9.14 \times 10^{-3}\,\mathrm{eV}$ per particle). The corresponding temperature dependence of the soft mode critical frequency, as well as of the relaxation are also shown in figure 4 in the ferroelectric SmC* and paraelectric SmA phases. The activation energy ($E_a = 78.88\ \mathrm{kJ\,mol^{-1}}$ or 0.73 eV per particle) in the ferroelectric SmC* phase at temperatures $T < T_c$ is almost twice the corresponding value obtained for the paraelectric SmA phase, i.e. at $T > T_c$ (where $E_a = 39.1\ \mathrm{kJ\,mol^{-1}}$ or 0.37 eV per particle). The ratio of the activation energies of these phases (SmA and SmC*), however, supports other results from previous measurements [25, 26]. This high value of the activation energy suggests that soft mode is a collective molecular possess and the high activation energy might be due to hindrance of rotation by the smectic potential. It is also seen from the dielectric spectra presented in figures 2 and 3 that the critical frequencies of the molecular relaxation are much higher than those obtained from the G-mode and S-modes. This result is consistent with the results from other similar materials [24, 25]. The activation energy obtained in this

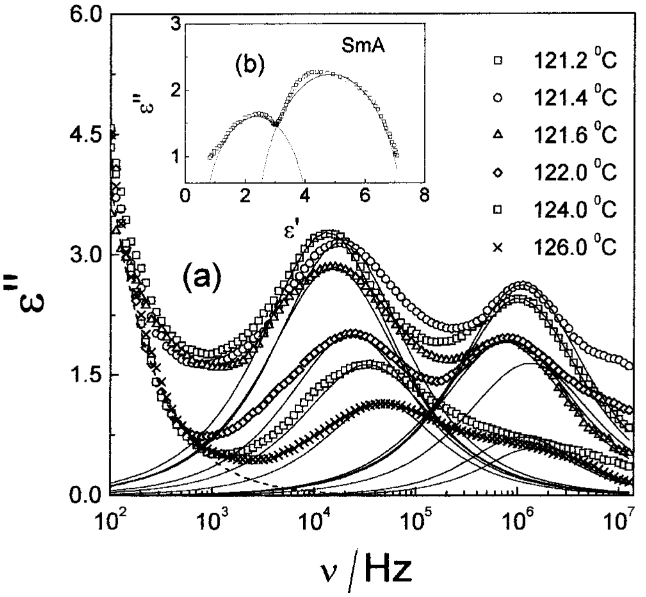

Figure 3. (*a*) Frequency (ν) dependence of the imaginary part of the dielectric constant (ε'') in the paraelectric SmA phase at different fixed temperatures. The solid line shows the conductivity contribution, (using equation (3), with the fit parameters $\delta_0 = 2.54 \times 10^{-11}\ \Omega^{-1}\,\mathrm{cm}^{-1}$ and $s = 0.067$). The solid line shows the Cole–Cole function, equation (2). (*b*) Cole–Cole plot obtained for the soft mode in the SmA phase.

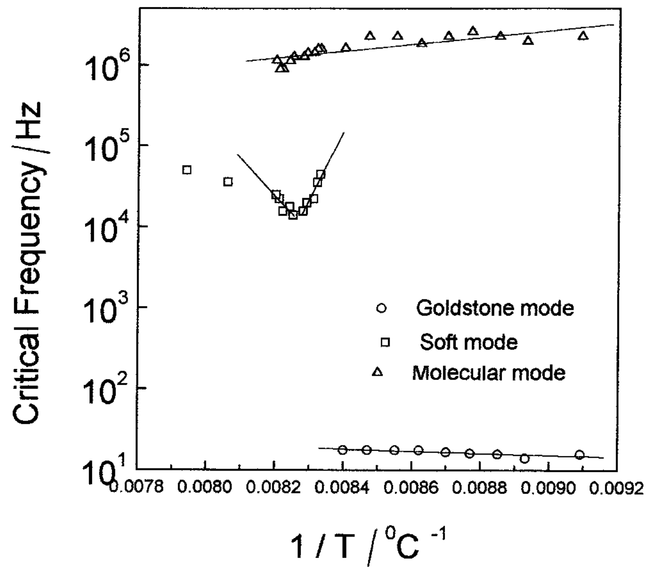

Figure 4. Variation of the critical frequency (ν_c) for the SmC* and SmA phases with temperature.

M-mode region is about 3.86 kJ mol^{-1} (0.3.62 × 10^{-2} eV per particle) which is, however, much lower than the values for other liquid crystalline materials [26, 27]. We suggest that this low value of the activation energy for the present sample is related to the rotational viscosity of the molecules (i.e. due to the high viscosity).

Figures 5 (*a*) and 5 (*b*) present, respectively, the thermal variation of the relaxation frequency and the inverse of the dielectric strength for the two collective modes. The characteristic 'V' shape of the soft mode behaviour in the vicinity of the SmA–SmC* transition is clearly seen from figure 5. This result can be explained using the molecular field approximation [22]. According to this approximation, the critical frequency of the soft mode should follow equation (4), and the slope ratio is predicted to be 2. The ratio of the slopes of the straight-line fits in figure 5 (*a*) is −2.34 for the relaxation frequency, about 17% higher than the corresponding theoretical value. Again the slope ratio for the inverse of the dielectric strength, figure 5(*b*), is −1.96, about 2% lower than the corresponding theoretical value. Hence, the frequency and the inverse of the dielectric strength of the soft mode extrapolated to the transition temperature at zero momentum transfer ($q = 0$) have a finite value and this supports the theory [22]. The two soft mode branches of the relaxation frequency in SmC* and SmA phases in the present FLC material meet at the Curie temperature $T_C = 120.85$°C which is about 0.15°C lower than the $T_C (= 121$°C$)$ observed from a texture study by polarizing optical microscopy. Similarly, the two soft mode branches of the inverse of the dielectric strength in the SmC* and SmA phases in the present FLC material meet at the Curie temperature $T_C = 121.2$°C which is about 0.2°C below the T_C (= 121°C) value observed from a texture study by microscopy. The very small differences in $T_C(\Delta T_C)$ between the texture and dielectric measurements may be taken to be within experimental error.

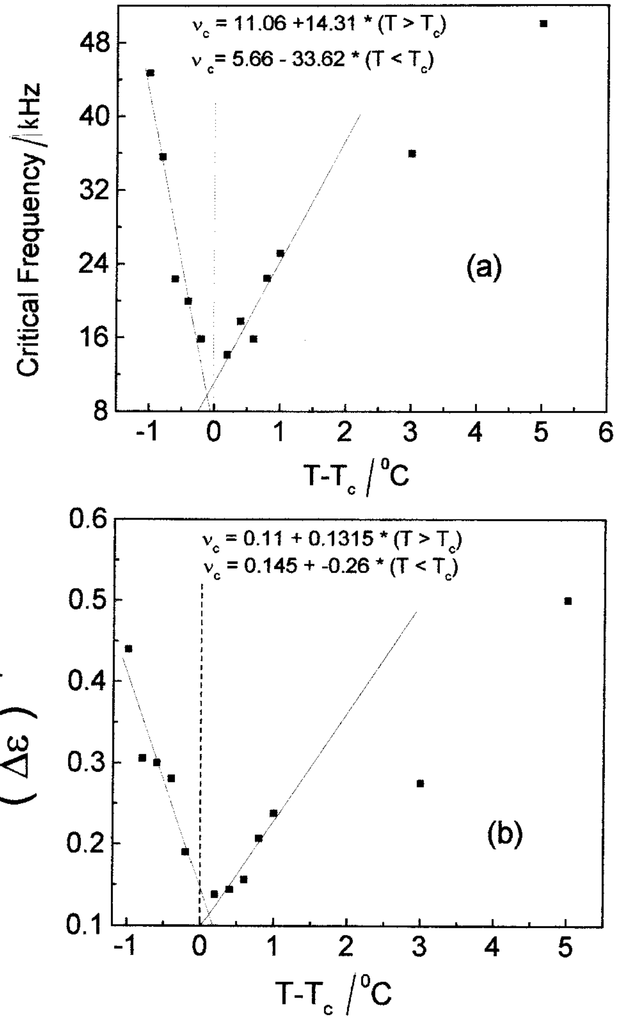

Figure 5. (*a*) Curie–Weiss plot of the S-mode critical frequency (ν_c) with temperature for the SmA and SmC* phases. (*b*) Curie–Weiss plot of the S-mode dielectric strength ($\Delta\varepsilon = \varepsilon_0 = \varepsilon_\alpha$) with temperature for the SmA and SmC* phases.

The effect of biasing voltage on the S-mode in the SmC* and SmA phases very close to the transition temperature ($T = 121$°C) has been studied using the planar aligned cell. The variation of the imaginary part of dielectric constant (ε'') with frequency with different bias voltages is shown in figure 6. The absorption in the SmC* and SmA phases of the S-mode contribution is suppressed on increasing the bias voltages. It is seen that at zero bias field, the dielectric permittivity (ε'') and the S-mode peak height are much stronger. By increasing the bias field, the S-mode strength decreases in both the phases, and the relaxation frequency increases. It is worth pointing out that the molecular relaxation exhibits a distribution of relaxation times, which is found to be consistent with the behaviour of other similar liquid crystalline materials [28, 29].

5. Conclusion

The temperature dependent dielectric relaxation properties of the FLCP studied (ferroelectric copolysiloxane (R)-COPS 11-10) are affected by the bias field. Under the bias field, the critical frequency shifts towards higher frequency while the dielectric strength gradually decreases. The low frequency G-mode obeys the Arrhenius law. It is noted that in the present sample, the S-mode can appear in both the SmC* and SmA phases (very close to the SmC*–SmA phase boundary). This behaviour supports the experimental, as well as the theoretical observations of Levstik *et al.* [16] in the case of an FLC mixture. Low frequency molecular relaxation is observed in both the smectic SmC* and SmA phases, and the activation energy in each relaxation mode was estimated by fitting the Arrhenius equation.

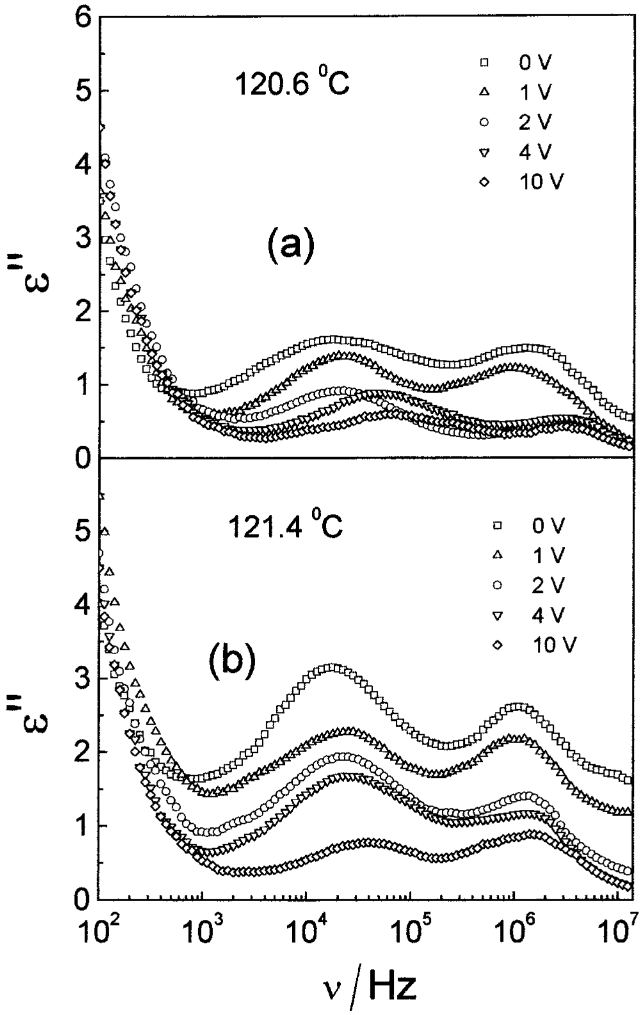

Figure 6. Frequency (ν) dependent imaginary part (ε'') of the dielectric constant near the transition temperature at different fixed bias fields for the SmC* (*a*) and SmA (*b*) phases.

B.K.C. is grateful to the AvH Foundation Germany and to Professor W. Haase for providing the instrumental facility for this work. S.K.K. is grateful to the CSIR, Government of India, for a research fellowship.

References

[1] Shibaev, P. V., Kozlowskii, M. V., Beresnev, L. A., Blinov, M. L., and Plate, N. A., 1984, *Polym. Bull.*, **12,** 299.
[2] Svensson, M., Helgee, B., Hjertberg, T., Hermann, D., and Skarp, K., 1993, *Polym. Bull.*, **31,** 167.
[3] Naciri, J., Pfeiffer, S., and Shashidhar, R., 1991, *Liq. Cryst.*, **10,** 585.
[4] Kitazume, T., Ohnogi, T., and Ito, J., 1990, *J. Am. chem. Soc.*, **112,** 6608.
[5] Uchida, S., Morita, K., Miyoshi, K., Kashimoti, K., and Kawasaki, K., 1988, *Mol. Cryst. liq. Cryst.*, **155,** 93.
[6] Zentel, R., Reckert, G., Sauvarop, B., and Kapitza, H., 1989, *Makromol. Chem.*, **190,** 2869.
[7] Meier, G., Sackmann, K., and Gragmaier, J. G., 1975, in *Applications of Liquid Crystals* (Springer), p. 150.
[8] De Jeu, W. H., 1978, *Solid State Physics Suppl.*, **14,** 109.
[9] Pfeiffer, M., Soto, G., Wròbel, S., Haase, W., Twieg, R., and Vetterton, K., 1991, *Ferroelectrics*, **21,** 55.
[10] Hiraoka, K., Taguchi, A., Ouchi, Y., Takezoe, H., and Fukuda, A., 1990, *Jpn. J. appl. Phys.*, **29,** L103.
[11] Gisse, P., Pavel, J., Nguyen, H. T., and Lorman, V. L., 1993, *Ferroelectrics*, **147,** 27.
[12] Isozaki, T., Suzuki, Y., Kawamura, I., Mori, K., Yamada, N., Orihara, H., and Ishibashi, Y., 1991, *Jpn. J. appl. Phys.*, **30,** L1570.
[13] Cepic, M., Heppke, G., Hollidt, J.-M., Lötzsch, D., and Zekš, B., 1993, *Ferroelectrics*, **147,** 159.
[14] Buivydas, M., Gouda, F., Lagerwall, S. T., and Stebler, B., 1995, *Liq. Cryst.*, **18,** 997.
[15] Musevic, O., Blinc, R., Zeks, B., Filipic, C., Copic, M., Seppen, A., Wyder, P., and Levanyuk, A., 1988, *Phys. Rev. Lett.*, **60,** 1530.
[16] Levstik, A., Carlsson, T., Filipic, C., Levstik, I., and Zekš, B., 1987, *Phys. Rev. A*, **35,** 3527.
[17] Mery, S., Catala, L., Sebastiao, P., Heinrich, B., Nicoud, J. F., and Guillon, D., 1999, *Liq. Cryst.*, 1999, **26,** 1445.
[18] Martin, J. A., Meier, G., and Saupe, A., 1971, *Symp. Faraday Soc.*, **5,** 119.
[19] Cole, K. S., and Cole, R. S., 1941, *J. Chem. Phys.*, **9,** 341.
[20] Hill, N. E., Vaughan, W. E., Price, A. H., and Davies, M., 1969, in *Dielectric Properties and Molecular Behavior* (New York: Von Nostrand Reinhold) pp. 49, 53 and 54.
[21] Mott, N. F., and Davis, E. A., 1979, *Electron Processes in Non Crystalline Materials*, 2nd Edn (Oxford: Clarendon Press).
[22] Blinc, R., and Zeks, B., 1978, *Phys. Rev. A*, **18,** 740.
[23] Biradar, A. M., Hiller, S., and Haase, W., 1995, *Ferroelectrics*, **173,** 267.
[24] Palacios, B., de Fuente, M. R., Perez Jubindo, M. A., and Ros, M. R., 1997, *Liq. Cryst.*, **23,** 349.
[25] Biradar, A. M., Wrobel, S., and Haase, W., 1989, *Phys. Rev. A*, **39,** 2693.
[26] Kresse, H., 1983, *Advances in Liquid Crystals*, Vol. 6, edited by G. H. Brown (New York: Academic Press), p. 109.
[27] Parneix, J. P., Legrand, C., and Decoster, D., 1983, *Mol. Cryst. liq. Cryst.*, **98,** 361.
[28] Hou, J., Schacht, J., and Gießelmaier, F., 1997, *Liq. Cryst.*, **22,** 409.
[29] Kocot, A., Wrzolik, R., Vij, J. K., Brehmer, M., and Zentel, R., 1994, *Phys. Rev. B*, **50,** 16 346.